Applied Environmental Research (2026) 48(1), 007
https://doi.org/10.35762/AER.2026007

Applied Environmental Research
- RESEARCH FOR SUSTAINABLE PLANET -

Research Article

Reduction of Cr(VI) with Infrared Light and Chemical Adsorption of Cr(III) by a God-Crown/Bentonite Composite for Electroplating Waste Remediation

Andre Taufik Kurniawan, Muhammad Djoni Bustan*, Sri Haryati

Department of Doctoral Engineering, Faculty of Engineering, Universitas Sriwijaya, Indonesia

*Corresponding Email: muhammaddjonibustan@ft.unsri.ac.id

Abstract

Heavy metal pollution, particularly chromium (Cr) from electroplating industrial waste, has severely threatened environmental quality and human health. This study aims to develop a composite adsorbent material based on bentonite and god crown biomass capable of removing chromium ions from liquid waste through a combination of reduction and adsorption mechanisms. The god crown/bentonite (GC/Bt) composite was synthesized at a mass ratio of 2:1 and calcined at 900°C. FTIR characterization revealed active functional groups (–OH, C=O, Si–O, and Al–O–Si), whereas BET analysis revealed a mesoporous structure (surface area 31.12 m^2 g^{-1}, pore diameter 4.37 nm) suitable for ion diffusion. The reduction of Cr(VI) to Cr(III) was facilitated by infrared (IR) irradiation, with 950 nm identified as the optimum wavelength compared with 730 nm. This conversion was confirmed by the significant increase in removal efficiency, as Cr(III) is more readily adsorbed by the composite than Cr(VI). The integrated system achieved a maximum removal efficiency (%R) of 86% and an adsorption capacity (q_e) of 703.19 mg g^{-1} under optimal continuous column conditions (bed height of 30 cm and flow rate of 4 L min^{-1}). The isotherm study showed the best fit with the Freundlich model, indicating a heterogeneous adsorbent surface, whereas the adsorption kinetics followed the pseudo-second-order model (R^2>0.97), indicating the dominance of the chemisorption mechanism. These results confirm that combining infrared reduction and chemical adsorption by GC/Bt composites is a practical approach for industrial chromium waste treatment.

ARTICLE HISTORY

Received: 25 Oct. 2025
Revised: 26 Jan. 2026
Accepted: 7 Feb. 2026
Published: 17 Feb. 2026

KEYWORDS

Chromium;
Bentonite;
God crown;
Adsorption;
Infrared reduction

Introduction

Water contamination from industrial effluents has emerged as a pressing global environmental concern, with sectors such as electroplating contributing significantly to this issue (Nguyen et al., 2021; Yang et al., 2023). Liquid waste from these operations is frequently contaminated with elevated concentrations of toxic heavy metals, particularly chromium (Cr), which is recognized as a nonbiodegradable pollutant with high toxicity (Lazaridis et al., 2005; Luna et al., 2021). An analysis of the data revealed that the electroplating process uses a minimal amount of Cr, approximately 30–40% of the total Cr. This leads to pollutants in the effluent with concentrations reaching 1,000 mg L^{-1}. The concentration of the substance in question in this body of water exceeds the maximum permissible limit established by the World Health Organization (WHO). The permissible limit for open water is 0.05 mg L^{-1}, as stipulated by the WHO (Rai et al., 2018; Senthilkumar et al., 2010). Exposure to Cr(VI) has been demonstrated to induce a range of deleterious health effects, including irritation and carcinogenic risks (Dula et al., 2014). This predicament is particularly pronounced in developing countries, where industrial waste is frequently disposed

of without adequate treatment (Dhungana and Yadav, 1970).

Although there are various wastewater treatment techniques, including chemical precipitation, ion exchange, and membrane methods, these approaches often face challenges such as high operational costs, significant secondary sludge generation, and complex implementation (Imran et al., 2020). As a result, research has shifted to adsorption as a more environmentally friendly, economical, easy-to-operate technology with high regeneration potential (Huang et al., 2019; Song et al., 2019; Tang et al., 2021). Various biomass-based materials have been explored (e.g., banana peel (Badessa et al., 2020), eggshells (Talukder et al., 2024), and tannin-rich biomass (Rajan et al., 2022; Shivshankar et al., 2024); however, generally, their low adsorption efficiency and long equilibrium contact times limit their application on an industrial scale. For example, previous studies using modified banana peels reported adsorption capacities of approximately 28–40 mg g^{-1} (Badessa et al., 2020), whereas eggshell-based composites typically achieved capacities of 40–90 mg g^{-1} (Talukder et al., 2024). Furthermore, unmodified bentonite often has a limited capacity (<20 mg g^{-1}) because of a lack of active binding sites (Slimani et al., 2025). These values are often insufficient to handle the high Cr concentrations in electroplating effluents, necessitating the development of materials with significantly higher capacity and faster kinetics.

To overcome the efficiency limitations inherent to conventional biomass adsorbents, this study adopted a hybrid material strategy that combines inorganic and organic components. The development of this novel adsorbent material involves the synthesis of two distinct materials endowed with complementary functionalities. Specifically, the combination incorporated bentonite clay minerals and god crown (*Phaleria macrocarpa*) biomass. Bentonite was selected for its high availability and superior structural properties. It has a large surface area and a high cation exchange capacity (CEC), primarily due to its montmorillonite content (Ilyas et al., 2021; Pawar et al., 2016; Rezvani et al., 2021; Slimani et al., 2025). These properties render it an ideal inorganic support. Conversely, the god crown was selected because of its elevated content of polyphenolic compounds, including tannins, which possess a strong chemical affinity for capturing heavy metal ions, such as Cr (Ahmad et al., 2023; Nasution et al., 2015) [21], [22]. This combination aims to create a synergistic material in which bentonite enhances the stability and surface area, whereas the god crown increases the chemical reactivity, thereby improving the adsorption capacity and efficiency.

In addition to developing composite materials, the pretreatment stage further enhances the Cr removal efficiency. The reduction of Cr(VI) to Cr(III) is a prerequisite because Cr(III) is much easier to adsorb and less toxic. Therefore, this study integrates the use of infrared (IR) light to facilitate the reduction of Cr(VI) to Cr(III) prior to adsorption. A combined strategy of active reduction via IR and chemical adsorption using a composite of a crown ether and bentonite is proposed as a comprehensive, highly efficient approach for the remediation of Cr waste.

The unique contribution of this study lies in the synergistic integration of specific IR irradiation with the engineered GC/Bt composite. Unlike conventional adsorption methods that rely solely on surface interactions, this hybrid approach utilizes IR energy, specifically at 950 nm, to actively destabilize and reduce Cr(VI) species. This photoreduction step serves as a catalyst, significantly accelerating the subsequent chemisorption of Cr(III) on the functionalized mesoporous surface of the composite. This dual-mechanism strategy addresses both the toxicity of the oxidation state and the kinetic limitations typically faced by single-stage biosorbents. Accordingly, the objectives of this study are twofold: first, to synthesize and characterize the GC/Bt composite, and second, to evaluate the performance of the IR-adsorption hybrid reduction process in removing Cr ions from aqueous solutions.

Materials and methods

1) Materials

The main component prepared was actual liquid waste from electroplating facilities, with Cr(VI) as the primary constituent. For the synthesis of composite adsorbent materials, two main precursors were used: a commercially available bentonite mineral from a chemical store in Palembang, Indonesia, and god crown fruit (*Phaleria macrocarpa*) from a local market in Palembang, Indonesia. All the solution preparation procedures, necessary dilutions, and overall adsorbent synthesis processes were carried out using deionized (distilled) water to ensure solvent purity.

2) Preparation of the GC/Bt composite adsorbent

The adsorbent preparation began with the preparation of god crown biomass. The fruit was washed, thinly sliced, and thermally dried until it reached a constant mass. This dry material is then pulverized and sieved through a 100-mesh sieve to obtain a uniform particle size distribution of approximately 150 μm. This particle size was selected to maximize the adsorption surface area while preventing column clogging during continuous-flow operations. Next, the composite adsorbent was synthesized by homogeneously mixing 100 g of god crown powder and 50 g of bentonite at a mass ratio of 2:1. Approximately 150 mL of distilled water was gradually added to the mixture while stirring continuously until it became plastic, and a homogeneous dough consistency suitable for pelletization was obtained.

This dough is then molded into cylindrical pellets. The critical activation stage was performed by calcination in a furnace. The temperature was increased from room temperature to 900°C at a heating rate of 10°C min^{-1} and held at this maximum temperature for 6 hours. This specific temperature and holding time were selected on the basis of the pyrolytic behavior of the biomass to ensure complete carbonization and structural stabilization of the bentonite matrix (Chen et al., 2012; Mesboua et al., 2021). Following the heating cycle, the samples were allowed to cool naturally to room temperature inside the furnace.

Furthermore, thermal treatment in this range facilitates the dehydroxylation of bentonite, transforming it into a more reactive phase without causing structural collapse. The absence of pore blockage was confirmed by BET analysis, which revealed a well-developed mesoporous network suitable for adsorption. Although this temperature typically induces combustion of organic matter, confinement of the crown biomass within the thermally resistant bentonite matrix facilitated carbonization rather than complete oxidation. This resulted in the formation of a stable carbonaceous structure (biochar) impregnated within the clay layers, preserving the critical oxygenated functional groups required for adsorption. This high-temperature thermal treatment was intended to improve the mechanical integrity of the pellets and activate surface adsorption sites. The calcined GC/Bt composite adsorbent was then stored in a desiccator to minimize the adsorption of atmospheric moisture before testing.

3) Reduction and adsorption experiments

The testing began by preparing a 10 L test solution by diluting concentrated electroplating industrial waste with distilled water. The initial concentration of Cr (C_0) in the test solution was determined to be 963 mg L^{-1}. To evaluate the effect of adsorbent dosage, the mass of the composite packed into the column was approximately 258 g for the small-diameter variation and 282 g for the large-diameter variation, resulting in a specific solution-to-adsorbent ratio determined by the column bed height (15 cm or 30 cm). The initial pH of the solution was adjusted to 3.0 ± 0.1 using 0.1 M HCl or NaOH, as the reduction of Cr(VI) is thermodynamically favorable under acidic conditions. The test solution then underwent a photoreduction pretreatment stage. This reduction process was carried out for 60 minutes by homogenizing the solution at 40°C and 75 rpm. The solution was irradiated via IR light with a power of 9 W at two different wavelengths, namely, 730 nm and 950 nm.

After pretreatment, the solution was fed into the adsorption system. Adsorption was carried out in continuous recirculation mode via adsorption columns with bed heights of 15 cm and 30 cm. The solution was recirculated through the column at a flow rate of 4–6 L min^{-1}. Samples were taken at 20-, 40-, and 60-minute intervals to monitor the adsorption kinetics. The residual Cr ion concentration in each sample was quantified via atomic absorption spectroscopy (AAS). All experimental runs were performed in triplicate to ensure reproducibility, and the data reported represent the average values. The standard deviation of the removal efficiency was less than 5%, indicating high experimental precision. Importantly, while AAS measures total Cr, the removal mechanism strongly implies a reduction. Hexavalent Cr (anionic $Cr_2O_7^{2-}$) has negligible affinity for the negatively charged bentonite-composite surface due to electrostatic repulsion. Therefore, the significant removal of total Cr observed confirms its conversion to the cationic trivalent form (Cr^{3+}), which is readily captured by the adsorbent's active sites.

The amount of Cr absorbed (q_e) at equilibrium on the GC/Bt composite adsorbent and the percentage of Cr removed from the solution were calculated via Eqs. 1 and 2 as follows:

$$q_e = ((C_0 - C_e)V)/m \quad \text{(Eq.1)}$$

$$\% = (C_0 - C_t)C_0 \times 100\% \quad \text{(Eq.2)}$$

The initial concentration of Cr in the test solution before the adsorption process is denoted as C_0 (mg L^{-1}). The concentration of Cr remaining in the solution after the system reached equilibrium was denoted as C_e (mg L^{-1}). The concentration at a specific time during kinetic testing is denoted as C_t (mg L^{-1}). The solution volume parameter used in the test is V (L), and m represents the mass of the composite adsorbent (g).

4) Adsorbent characterization

The physical and chemical characteristics of the GC/Bt composite adsorbent were analyzed via two spectroscopy methods and gas adsorption techniques. The surface textural properties of the adsorbent, including specific surface area, pore volume, and pore size distribution, were determined through Brunauer–Emmett–Teller (BET) analysis. The BET test was performed via a Quantachrome Instruments NOVA Touch 4LX instrument on the basis of nitrogen gas adsorption–desorption isotherms at 77 K. To identify the functional groups directly involved in the chemisorption mechanism of Cr^{3+} ions, Fourier transform infrared (FTIR) spectroscopy analysis was performed. FTIR analysis was carried out via a Perkin Elmer Spectrum Two System L160000A instrument, with spectra obtained over a specific wavelength range to verify chemical bond vibrations on the adsorbent surface.

Results and discussion

1) Characterization of the GC/Bt composite adsorbent

The FTIR analysis was performed to identify critical functional groups on the GC/Bt composite adsorbent, thereby verifying the ability of the adsorbent to chemisorb Cr^{3+} ions (Figure 1). The obtained spectrum showed characteristic absorption from organic (god crown/lignin) and inorganic (bentonite) components. The broad and strong absorption band at 3,283.66 cm^{-1} indicates the presence of O-H stretching from phenolic and carboxyl hydroxyl groups. These groups are significant because they are the main active sites that undergo deprotonation (O- or COO-) and provide anionic sites capable of forming stable chemical coordination bonds (chemisorption) with Cr^{3+} cations (Chen et al., 2012; Mesboua et al., 2021). Additionally, the absorption peak at 1,619.64 cm^{-1} corresponds to the C=O extension from the carbonyl or ionized carboxylate group, which is also a strong chemical absorption site (Belachew et al., 2020; Bougda et al., 2020). The presence of bands at 1,019.34 cm-1 and below 600 cm^{-1} definitively confirms that the inorganic bentonite matrix (Si–O and Al–O–Si) acts as a structural support, supporting the material through a secondary cation exchange mechanism (Fink et al., 2021; Kostryukov et al., 2023)]. These FTIR results strongly support the proposed chemisorption mechanism, indicating that the GC/Bt composite possesses the functional groups necessary to efficiently remove Cr^{3+} ions.

The surface texture of the GC/Bt composite was characterized via nitrogen adsorption–desorption analysis at 77 K; the results are shown in Figure 2a. The isotherm curve is type IV with a hysteresis loop, indicating a mesoporous structure. This suggests that the material combines micro- and mesopores, thereby increasing its adsorption capacity. The BET calculations revealed a specific surface area of 31.12 $m^2\ g^{-1}$, a total pore volume of 0.0340 $cm^3\ g^{-1}$, and an average pore diameter of 4.37 nm. These values confirm that the GC/Bt composite is a mesoporous material with pores ranging from 2 to 50 nm. The relatively small pore volume indicates that part of the bentonite surface has been covered by organic molecules from the god crown, which causes a decrease in pore accessibility compared with that of pure bentonite. This is consistent with the tendency to decrease the surface area due to interactions between organic functional groups (–OH and C=O) from god crown lignin and Si–O and Al–O–Si groups in bentonite.

The BET plot (inset in Figure 2b) shows a linear relationship between $(1/[W((P/P_0)-1])$ and relative pressure (P/P_0) in the range of 0.05–0.30, which is consistent with the BET model and produces a high correlation coefficient (R^2) value (0.96), indicating measurement accuracy. These results suggest that the combination of god crowns with bentonite produces a composite material with stable mesopore porosity and a moderate surface area, potentially improving the adsorption capacity for Cr waste.

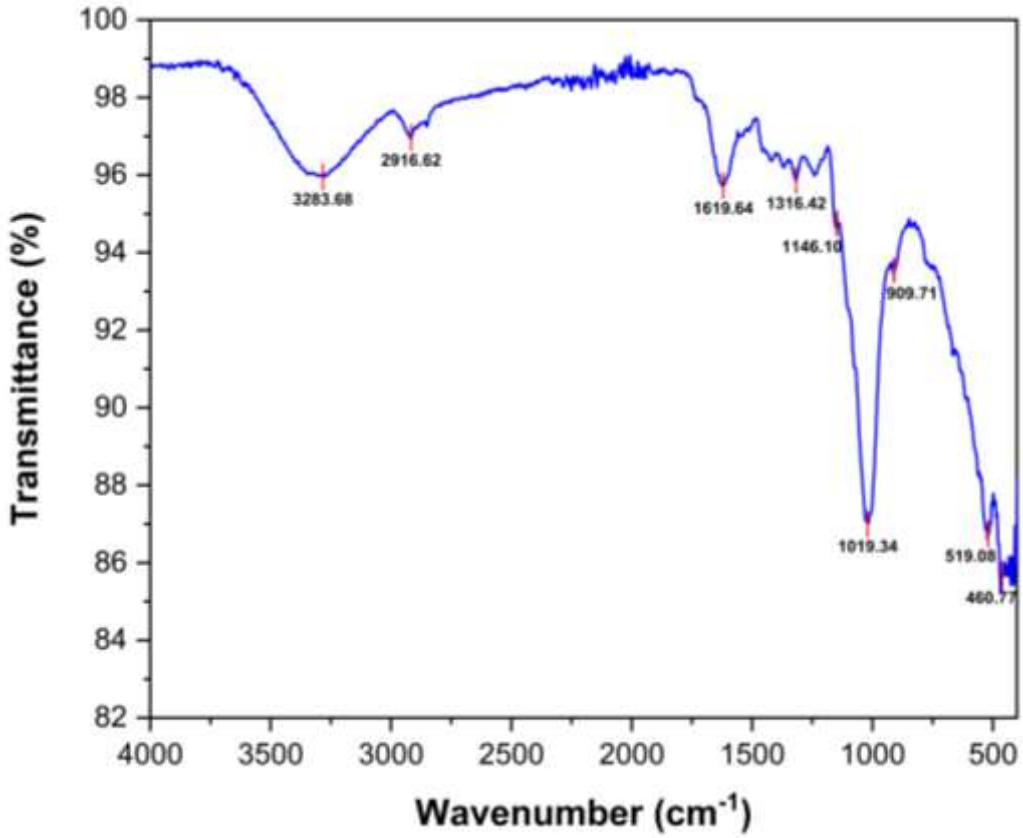

Figure 1 Functional group characteristics of the GC/Bt composite based on FTIR analysis.

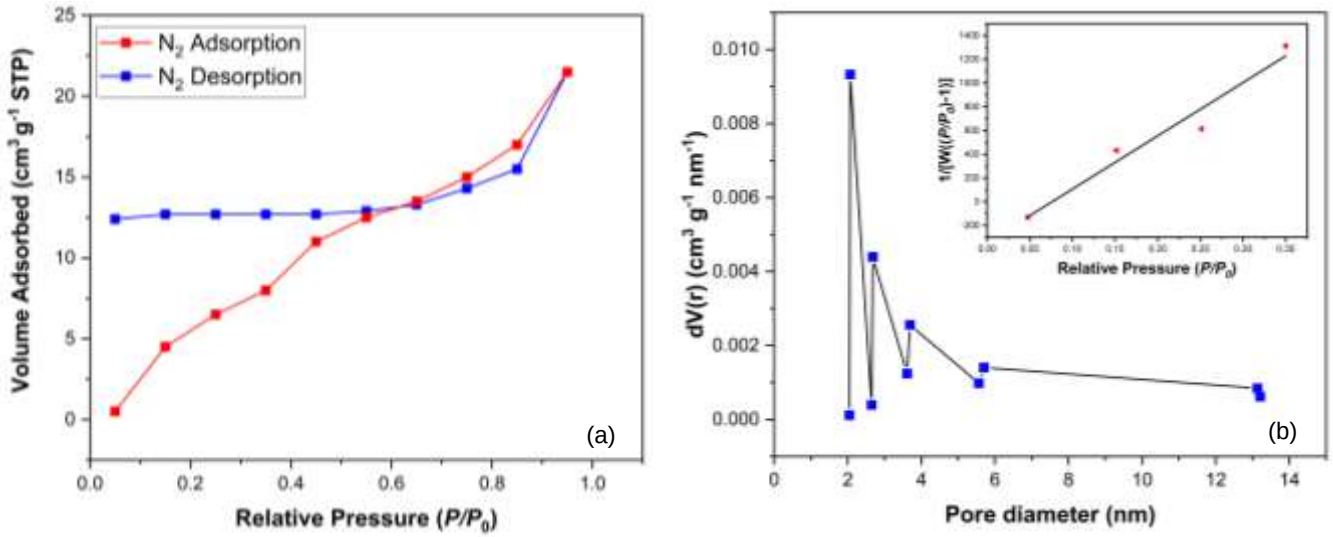

Figure 2 BET analysis of the GC/Bt composite surface: a) isotherm profile and b) pore size profile.

2) Adsorption of Cr on GC/Bt

The data in Figures 3 and 4 show that Cr(III) adsorption onto the GC/Bt composite adsorbents effectively removes Cr from liquid waste. The removal efficiency is significantly influenced by several operational parameters, namely, the flow rate, bed height, adsorbent diameter, and infrared wavelength used for reduction. The graph shows that the adsorption efficiency generally increases with increasing contact time. This increase is consistent across all the variations, indicating that the adsorption process continues as the Cr ions interact with the active sites on the adsorbent surface. The highest peak efficiency was achieved at a contact time of 60 minutes.

The results of this study clearly show that a bed height of 30 cm (H30) and a lower flow rate of 4 L min $^{-1}$ (F4) are the optimal conditions for achieving maximum removal efficiency. The H30 condition provides more active sites because of the larger adsorbent volume, whereas the lower flow rate (F4) prolongs the retention time of the waste in the bed. This longer contact time gives Cr ions a greater opportunity to diffuse from the liquid phase and attach to the adsorbent surface. Conversely, at a higher flow rate (F6), the short contact time causes Cr ions to pass through the bed quickly, limiting interaction with the adsorbent and resulting in a lower removal percentage.

The diameter of the adsorbent also plays a crucial role in the adsorption efficiency. The data show that adsorbents with smaller diameters (S = 0.965 cm) consistently provide higher adsorption capacities and removal percentages than those with larger diameters (B = 1.287 cm). This observation is consistent with mass transfer principles; smaller diameters have a larger specific surface area, directly increasing the number of active sites available per unit mass of adsorbent. In addition, the shorter diffusion distance within the 0.965 cm pellets facilitates the mass transfer of Cr(III) ions from the solution to the adsorbent surface and its internal pores, accelerating adsorption and increasing overall efficiency.

Interestingly, an inverse relationship was observed between the adsorption capacity (Figure 3) and removal efficiency (Figure 4a). Sample F6H15-730S exhibited the highest adsorption capacity (q_e), whereas sample F4H15-730S (yellow line) demonstrated the highest percentage removal. This phenomenon is attributed to the effects of the flow rate and residence time. At a higher flow rate (F6), the mass loading of Cr ions per unit time increases, increasing the concentration gradient and driving force for adsorption, which results in a higher calculated uptake capacity (q_e). Conversely, at the lower flow rate (F4), the solution residence time within the column is longer, allowing for more complete interaction between the adsorbate and the active sites, thereby yielding a cleaner effluent and a higher removal efficiency (%) despite the lower total mass loading rate.

One of the most significant findings of this study is the effect of the infrared wavelength on system performance. A comparison of the data at 730 nm and 950 nm shows that the process at 950 nm generally yields higher removal percentages and adsorption capacities. Infrared light at specific wavelengths can induce molecular vibrations that effectively break the Cr-O bonds in Cr(VI) ions, facilitating their reduction to Cr(III), which is more easily adsorbed by the adsorbent. The better performance at 950 nm indicates that this wavelength lies within the optimal energy-absorption range for the reduction reaction, thereby increasing the concentration of Cr(III), which the bentonite-gold crown composite adsorbent can efficiently remove. This process highlights the advantages of the hybrid approach, in which the reduction step enhances the adsorption efficiency, providing a comprehensive solution for Cr waste treatment.

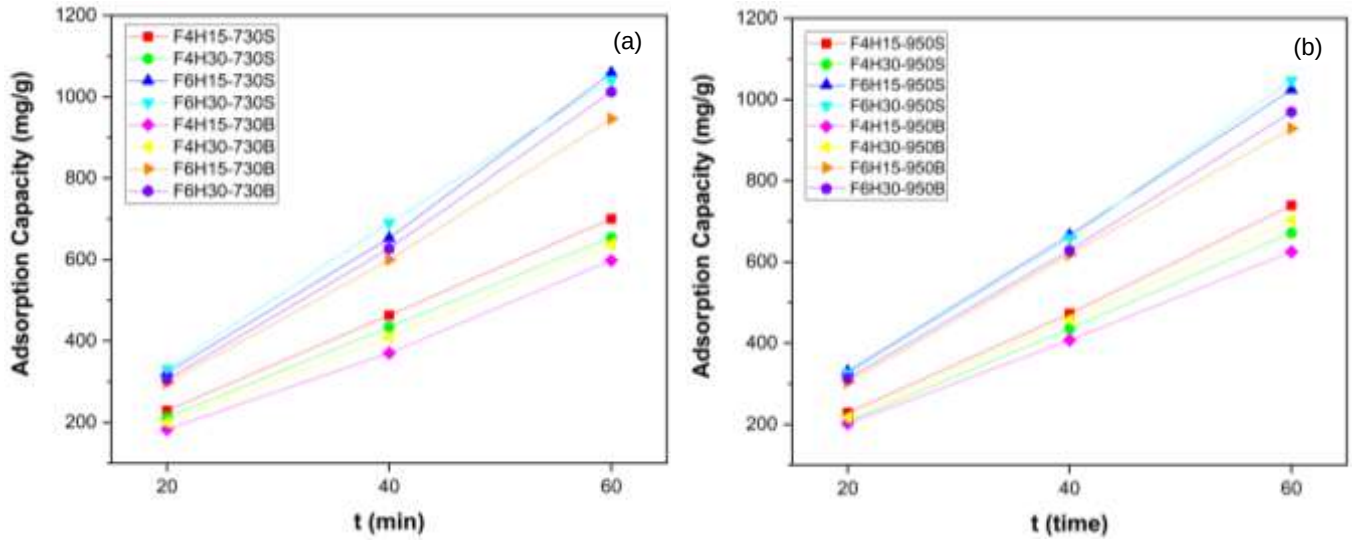

Figure 3 Adsorption capacity at various wavelengths: a) 730 nm and b) 950 nm. (Flow rates: F4 = 4 L min^{-1} and F6 = 6 L min^{-1}; bed heights: H15 = 15 cm and H30 = 30 cm; diameters: S = 0.965 cm and B = 1.287 cm).

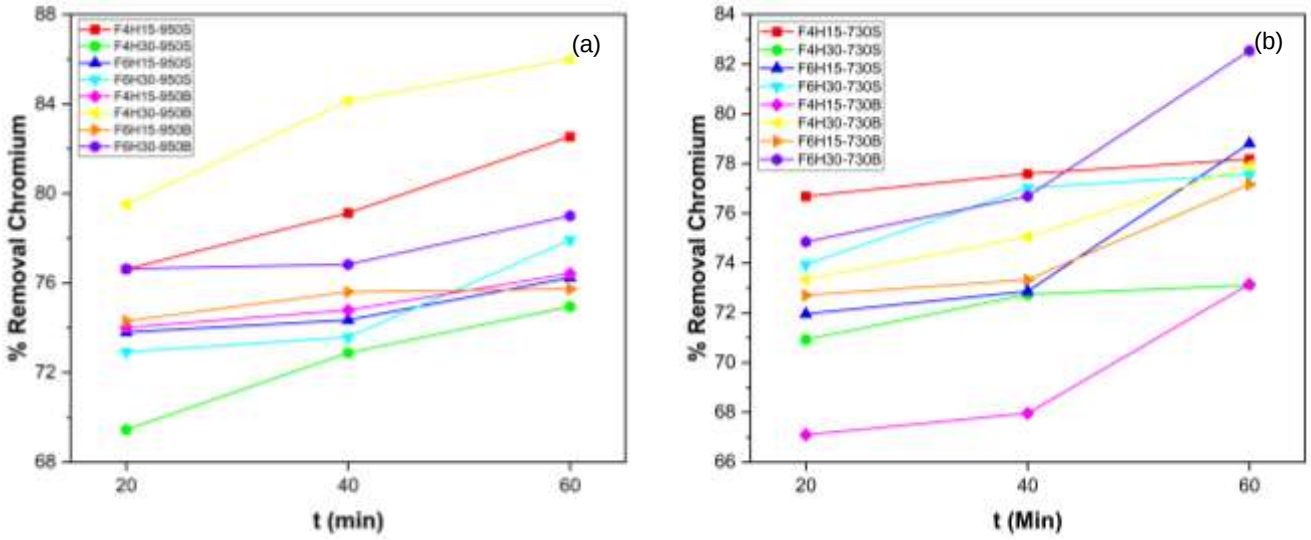

Figure 4 % Removal of Cr at various wavelengths: a) 730 nm and b) 950 nm. (Flow rates: F4 = 4 L min^{-1} and F6 = 6 L min^{-1}; bed heights: H15 = 15 cm and H30 = 30 cm; diameters: S = 0.965 cm and B = 1.287 cm).

3) Adsorption isotherm study

The isothermal adsorption experiment on GC/BT was conducted at T = 40°C, with variations in the flow rate, bed height, adsorbent diameter, and wavelength. The experimental data obtained were analyzed via the Langmuir and Freundlich linear isotherm models (Tabak et al., 2011), which are given by Eqs. 3 and 4.

Langmuir equation:

$$C_e/q_e = (1/q_m)C_e + (1/q_m K_L) \qquad \text{(Eq.3)}$$

Freundlich equation:

$$\log(q_e) = (1/n)\log(C_e) + \log(K_F) \qquad \text{(Eq.4)}$$

where q_e (mg g^{-1}) is the amount absorbed by the adsorbent at equilibrium, C_e (mg L^{-1}) is the equilibrium concentration of Cr, K_L is the Langmuir constant, and K_F and n are the Freundlich constants. Adsorption isotherm analysis was performed to elucidate the interaction mechanism between the adsorbate, namely, (Cr(III)) ions, and the GC/Bt composite adsorbent under equilibrium conditions. On the basis of the data presented, the adsorption process was evaluated for its suitability with the two most common isotherm models, namely, the Langmuir and Freundlich models. The results showed that the experimental data could be explained by both models, albeit with varying degrees of correlation.

The Langmuir model assumes monolayer adsorption on a homogeneous surface. Several operational conditions showed excellent fits with this model, as indicated by coefficient of determination (R^2) values approaching 1.0 for F6H15-730S (R^2 = 0.9967) and F6H15-950B (R^2 = 0.9907) (Figure 5 and Table 1). This strong correlation indicates that under these conditions, Cr(III) adsorption

predominantly occurs at uniform active sites, forming a single layer.

Conversely, the Freundlich model, which describes multilayer adsorption on heterogeneous surfaces, shows a superior fit under other conditions. This is evident from the higher R^2 values for conditions F4H15-730S (R^2 = 0.99875) and F6H15-950S (R^2 = 0.99882) than for the Langmuir model (Figure 6 and Table 1). This better fit supports the hypothesis that the composite adsorbent surface is heterogeneous, offering a range of adsorption sites with different energies. This heterogeneity most likely arises from the combination of bentonite, which is rich in ion-exchange sites and cations and provides organic functional groups. The qualitative interpretation of the R^2 value strongly supports the hypothesis that Cr adsorption involves a dual mechanism. The Freundlich model is more appropriate for most variations, indicating the importance of surface heterogeneity in this adsorption mechanism. This suggests a synergy between the chemical and physical properties of the two adsorbent components.

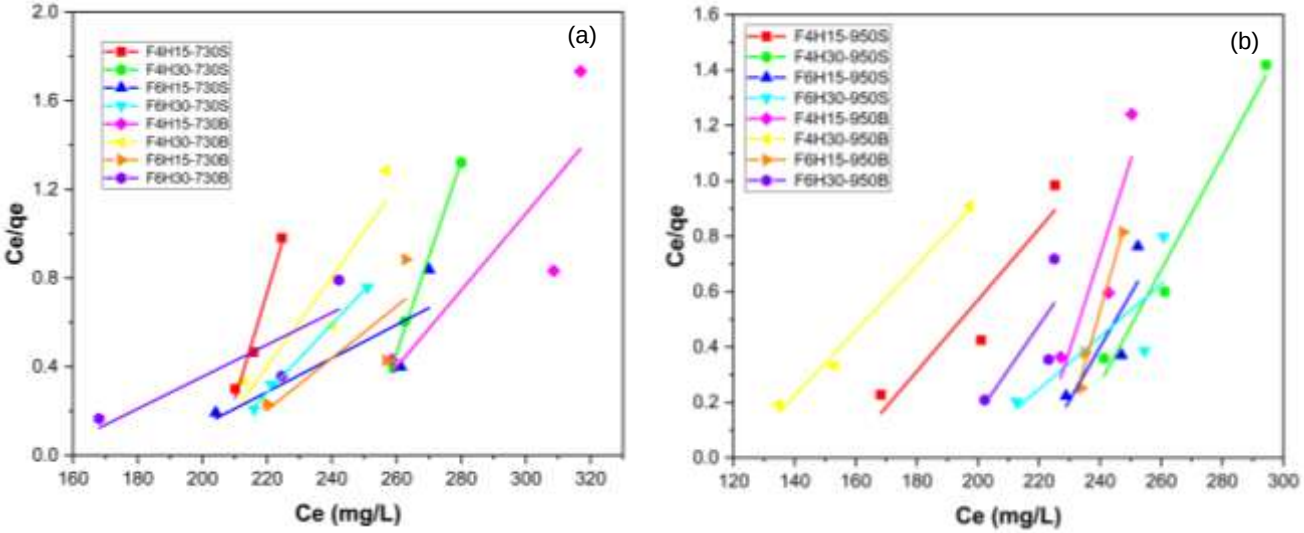

Figure 5 Linearization curve of the Langmuir isotherm for Cr(III) adsorption on the GC/Bt composite on the basis of wavelength variation: a) 730 nm and b) 950 nm.

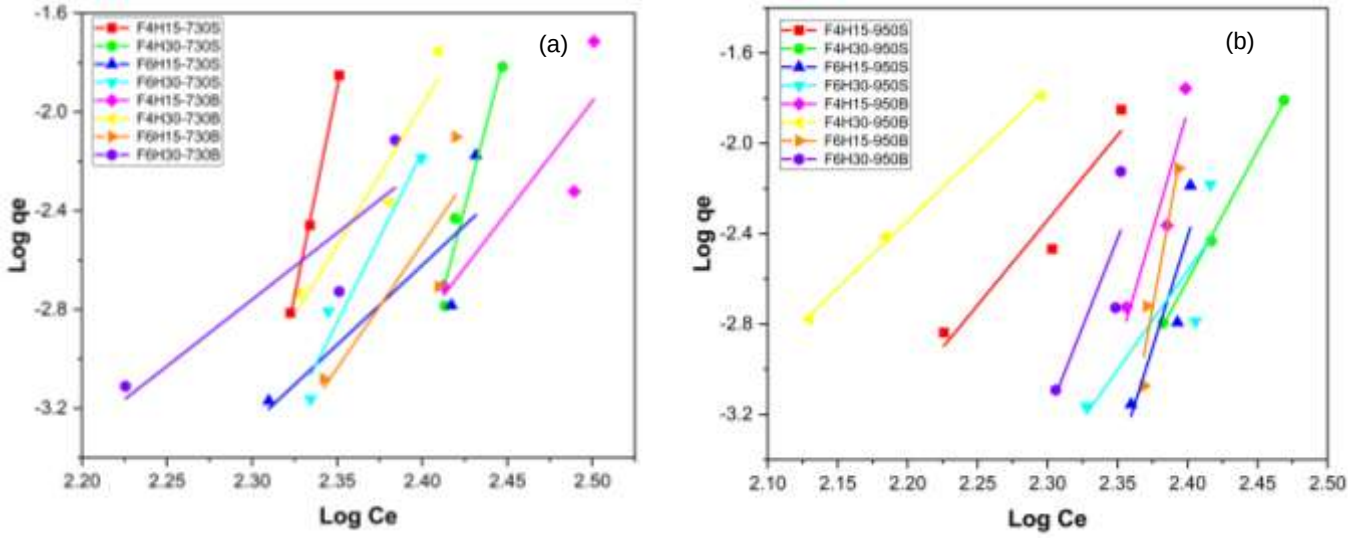

Figure 6 Linearization curve of the Freundlich isotherm for Cr(III) adsorption on the GC/Bt composite on the basis of wavelength variation: (a) 730 nm and (b) 950 nm.Linearization curve of the Freundlich isotherm for Cr(III) adsorption on the GC/Bt composite on the basis of wavelength variation: (a) 730 nm and (b) 950 nm.

Table 1 Langmuir and Freundlich isotherm parameters for Cr(III) adsorption by the GC/Bt composite under various operating conditions

Variation	Langmuir			Freundlich		
	q_m (mg g^{-1})	K_L (L mg^{-1})	R^2	K_F (L mg^{-1})	1/n	R^2
F4H15-730S	0.0483	0.0049	0.9732	1.4E-81	33.6011	0.99875
F6H15-730S	0.0432	0.0040	0.9967	2.0E-67	26.5178	0.95813
F4H30-730S	0.0076	0.0055	0.6775	8.0E-19	6.4491	0.73261
F6H30-730S	0.0154	0.0050	0.9968	6.5E-36	13.7602	0.95288
F4H15-730B	0.0173	0.0042	0.6727	3.9E-25	8.9803	0.74276
F6H15-730B	0.0207	0.0051	0.8436	6.3E-30	11.3457	0.90683
F4H30-730B	0.0117	0.0049	0.6617	2.1E-27	10.0624	0.73555
F6H30-730B	0.0072	0.0066	0.7597	6.8E-16	5.3938	0.80520
F4H15-950S	0.0129	0.0064	0.8788	2.3E-20	7.5212	0.92916
F6H15-950S	0.0205	0.0044	0.9738	6.9E-31	11.4827	0.99882
F4H30-950S	0.0192	0.0046	0.7162	2.3E-50	19.6779	0.80464
F6H30-950S	0.0095	0.0052	0.6607	2.7E-24	8.7486	0.72914
F4H15-950B	0.0343	0.0046	0.7991	1.9E-53	21.1961	0.87885
F6H15-950B	0.0118	0.0083	0.9907	4.1E-16	5.9266	0.99828
F4H30-950B	0.0385	0.0044	0.9816	1.9E-84	34.1006	0.92081
F6H30-950B	0.0160	0.0053	0.5955	5.3E-40	15.6834	0.68679

4) Kinetic adsorption study

The kinetic experiments were conducted in triplicate to ensure data reproducibility. The results presented are averages, with standard deviations consistently less than 5%, indicating high precision and minimal experimental error. An in-depth analysis of the existing kinetic data was conducted via pseudo-first-order (PFO) and pseudo-second-order (PSO) models to facilitate a comprehensive understanding of the parameters governing the adsorption process. The PFO model, which is generally associated with physisorption processes, was analyzed via the following linear equation (Eq.5) (Belbachir and Makhoukhi, 2017).

$$\log(q_e - q_t) = \log q_e - (k_t/2.303)t \qquad \text{(Eq.5)}$$

Concurrently, testing of the PSO model, often referred to as an indicator of chemical adsorption as a rate-determining step, was performed via Eq.6 (Degefu and Dawit, 2013).

$$1/q_t = (1/k_2 q_e^t) + (1/q_t)t \qquad \text{(Eq.6)}$$

Adsorption kinetics studies are crucial for understanding the rate of the process and the mechanisms that control it, whether it is external mass transfer, intraparticle diffusion, or surface chemical interactions. On the basis of the data presented (Table 2), the adsorption kinetics of Cr(III) on the GC/Bt composite were evaluated via PFO and PSO models. The results indicate a significant discrepancy between the two models. The PFO model exhibited relatively low correlation coefficients ($R^2 \approx 0.78$) and yielded theoretical adsorption capacity values (q_e,calc) that were excessively high and inconsistent with experimental observations (q_e,exp). This poor fit suggests that the adsorption process is not governed by the physical mechanisms typically associated with the first-order model.

In contrast, the PSO model demonstrated an excellent fit to the experimental data, with high determination coefficients ($R^2 > 0.97$). Furthermore, the recalculated q_e,calc values for the PSO model were found to be in close agreement with the experimental values (q_e,exp), ranging from 620 to 1,100 mg g^{-1}. This strong consistency indicates that the adsorption rate is primarily controlled by chemisorption, which involves electron sharing or exchange between the Cr ions and the composite's functional groups, rather than by mass transfer alone.

5) Mechanism of Cr(VI) reduction to Cr(III) with infrared light and chemisorption of Cr(III) by GC/Bt

On the basis of the removal efficiency and kinetic data, a dual-stage mechanism involving the reduction of Cr(VI) followed by the chemisorption of Cr(III) is proposed. Although direct spectral monitoring of the Cr(VI) species concentration was not performed, the reduction pathway is strongly supported by surface-chemistry logic.

The GC/Bt composite surface is predominantly negatively charged under operating conditions because of ionized hydroxyl and silanol groups. Theoretically, this surface would electrostatically repel anionic hexavalent Cr ($Cr_2O_7^{2-}$ or $HCrO^{4-}$), leading to negligible adsorption. However, the experimental results revealed significant removal of total Cr. This observation implies that anionic Cr(VI) is likely reduced to the cationic trivalent form (Cr^{3+}), which is then attracted to the adsorbent surface. The enhanced performance under 950 nm IR irradiation further supports the hypo-thesis that photon energy facilitates this reduction step, enabling subsequent chemisorption by the composite's functional groups.

The initial stage of this treatment process is a redox reaction initiated by photon energy from IR light, aimed at converting highly toxic hexavalent Cr (Cr(VI)) into a relatively stable, easily removable trivalent form (Cr^{3+}). IR light serves as essential activation energy, facilitating the necessary electron transfer. The main reduction reaction takes place in an acidic environment, where dichromate ions ($Cr_2O_7^{2-}$) consume six electrons and react with hydrogen ions (H^+) to produce soluble Cr^{3+} ions and water molecules, as illustrated in Eq.7.

The research data highlight the importance of specific wavelengths, with optimal performance at 950 nm, indicating that photons at this frequency efficiently trigger Cr–O bond vibrations in dichromate ions, thereby thermodynamically facilitating the reduction process. The result of this stage is the availability of Cr^{3+} ions in solution, which become the ideal substrate for the chemical adsorption mechanism in the next stage.

The second stage immediately follows reduction and focuses on removing dissolved Cr^{3+} ions from the system via strong chemisorption by the GC/Bt composite adsorbent. This process was confirmed by kinetic findings that showed a superior fit with the PSO model, indicating that the adsorption rate was controlled by chemical reactions involving valence bond formation. Lignin from the composite serves as the primary adsorption agent, providing electron-rich functional groups such as carboxylate (R-COO-) and phenolate (R-O-). Cr^{3+} ions (as Lewis acids) then interact strongly with these anionic groups (as Lewis bases) to form stable surface coordination complexes, as generally illustrated in Eqs. 8 and 9.

The stability of this bond, which exceeds that of physical adsorption interactions, ensures the effective and permanent removal of Cr^{3+}. The stronger fit of the isotherm to the Freundlich model also indicates that chemisorption occurs on a heterogeneous surface, reflecting the synergy between specific binding sites (lignin) and the ion exchange capacity (bentonite) in securing Cr^{3+} ions.

Table 2 Adsorption kinetic parameters of Cr(III) by the GC/Bt composite based on pseudo-first-order and pseudo-second-order models

Variation	$q_{e,\,exp}$ (mg g^{-1})	PFO			PSO		
		$q_{e\,(calc)}$ (mg g^{-1})	k_1 (min^{-1})	R^2	$q_{e\,(calc)}$ (mg g^{-1})	k_1 (min^{-1})	R^2
F4H15-730S	700.28	2,269.66	0.4685	0.7894	715.50	0.000025	0.99987
F6H15-730S	1,058.88	2,040.47	0.4663	0.7901	1,085.20	0.000019	0.99997
F4H30-730S	654.82	4,926.63	0.4845	0.7830	672.10	0.000007	0.97429
F6H30-730S	1,042.29	4,483.01	0.4822	0.7890	1,075.00	0.000013	0.99986
F4H15-730B	739.27	2,626.58	0.4639	0.7848	758.80	0.000007	0.98520
F6H15-730B	1,024.28	2,220.50	0.4658	0.7875	1,050.65	0.000009	0.99419
F4H30-730B	671.37	4,362.24	0.4800	0.7850	695.90	0.000008	0.98804
F6H30-730B	1,046.94	4,709.45	0.4830	0.7837	1,075.30	0.000007	0.97031
F4H15-950S	598.09	1,891.52	0.4713	0.7848	615.55	0.000008	0.98963
F6H15-950S	946.43	2,027.54	0.4679	0.7875	970.25	0.000008	0.99891
F4H30-950S	637.14	3,949.57	0.4823	0.7850	655.80	0.000014	0.99694
F6H30-950S	1,012.35	4,577.31	0.4837	0.7837	1,040.10	0.000008	0.98460
F4H15-950B	624.81	1,909.28	0.4646	0.7885	645.75	0.000014	0.99792
F6H15-950B	928.79	2,392.71	0.4696	0.7893	955.40	0.000010	0.99852
F4H30-950B	703.19	3,619.35	0.4786	0.7892	725.50	0.000029	0.99991
F6H30-950B	968.94	3,978.41	0.4803	0.7866	995.60	0.000014	0.99438

$$Cr_2O_7^{2-} + 14H^+ + 6e^- \xrightarrow{IR\ (h\nu)} 2Cr^{3+} + 7H_2O \quad \text{(Eq.7)}$$

$$\text{Lignin–R–COO}^-_{(ads)} + Cr^{3+}_{(aq)} \leftrightarrow \text{Lignin–R–COO–}Cr^{2+}_{(ads)} \quad \text{(Eq.8)}$$

$$\text{Lignin–R–O}^-_{(ads)} + Cr^{3+}_{(aq)} \leftrightarrow \text{Lignin–R–O–}Cr^{2+}_{(ads)} \quad \text{(Eq.9)}$$

Conclusions

This study successfully developed a composite material based on a god crown and bentonite biomass as a hybrid adsorbent for Cr waste treatment. FTIR and BET characterization revealed that the GC/Bt composite possessed active functional groups (–OH, C=O, Si–O, and Al–O–Si) and a mesoporous structure with a surface area of 31.12 m^2 g^{-1}, which supported the metal ion adsorption process.

The experimental results suggest that the reduction stage using IR light facilitates the conversion of toxic Cr(VI) into more easily adsorbed Cr(III) species. A wavelength of 950 nm was found to be most effective in enhancing removal efficiency, likely because the photon energy accelerates the reduction process.

Isotherm analysis indicated that the Freundlich model was the most suitable model, indicating the heterogeneous nature of the adsorbent surface. Moreover, kinetic studies revealed the best fit with the pseudo-second-order model, indicating that the adsorption mechanism is controlled by chemisorption.

However, it is essential to acknowledge the limitations of this study. While the high removal efficiency implies successful reduction, direct surface speciation analysis (e.g., XPS or UV–Vis) to quantify the exact ratio of reduced Cr(VI) was not performed. Additionally, the reusability of the adsorbent was not evaluated in this work. Future studies should focus on spectroscopic validation of the reduction mechanism and conduct regeneration cycles to assess the composite's long-term industrial viability. Overall, the combination of IR photoreduction and chemical adsorption by the GC/Bt composites has potential as an efficient approach for chromium remediation.

Data availability statement

Information and data used in the study will be disclosed upon request.

Author ORCID

Andre Taufik Kurniawan: 0009-0008-4300-2408
Muhammad Djoni Bustan: 0009-0008-7742-0296
Sri Haryati: 0000-0002-7490-6118

Author contributions

Andre Taufik Kurniawan: Methodology, Software, Validation, Formal analysis, Investigation, Resources, Data curation, Writing – Original draft, Writing – Review & Editing, Project administration, Funding acquisition
Muhammad Djoni Bustan: Conceptualization, Methodology, Visualization, Supervision
Sri Haryati: Conceptualization, Methodology, Visualization, Supervision

Conflicts of interest

The authors declare that there are no conflicts of interest in competing financial or personal relationships that could have appeared to influence the work reported in this work.

References

Ahmad, R., Mazlan, M. K., N., Aziz, A. F., A., Gazzali, A. M., Rawa, M. S., A., & Wahab, A. H. (2023). Phaleria macrocarpa (Scheff.) Boerl.: An updated review of pharmacological effects, toxicity studies, and separation techniques. *Saudi Pharmaceutical Journal*, *31*(6), 874–888

Badessa, T. S., Wakuma, E., & Yimer, A. M. (2020). Bio-sorption for effective removal of chromium(VI) from wastewater using Moringa stenopetala seed powder (MSSP) and banana peel powder (BPP). *BMC Chemistry*, *14*(1), 71.

Belachew, N., & Hinsene, H. (2020). Preparation of cationic surfactant-modified kaolin for enhanced adsorption of hexavalent chromium from aqueous solution. *Applied Water Science*, *10*(1), 38.

Belbachir, I., & Makhoukhi, B. (2017). Adsorption of Bezathren dyes onto sodic bentonite from aqueous solutions. *Journal of the Taiwan Institute of Chemical Engineers*, *75*, 105–111.

Bougdah, N., Messikh, N., Bousba, S., Magri, F. D. P., & Rogalski, M. (2020). Removal of chlorobenzene by adsorption from aqueous solutions on the HDTMA-bentonites as a function of HDTMA/CEC ratio. *Current Research in Green and Sustainable Chemistry*, *3*, 100038.

Chen, Y. Yang, H., Wang, X., Zhang, S., & Chen, H. Biomass-based pyrolytic polygeneration system on cotton stalk pyrolysis: Influence of temperature. *Bioresource Technology*, *107*, 411–418.

Degefu, D. M., & Dawit, M. (2013). Chromium removal from modjo tannery wastewater using Moringa stenopetala seed powder as an adsorbent. *Water, Air, & Soil Pollution*, *224*(12), 1719.

Dhungana, T. P., & Yadav, P. N. (1970). Determination of chromium in tannery effluent and study of adsorption of Cr (VI) on saw dust and charcoal from sugarcane bagasses. *Journal of Nepal Chemical Society*, *23*, 93–101.

Dula, T., Siraj, K., & and Kitte, S. A. (2014). Adsorption of hexavalent chromium from aqueous solution using chemically activated carbon prepared from locally available waste of bamboo (Oxytenanthera abyssinica). *ISRN Environmental Chemistry*, *2014*, 1–9.

Fink, F., Emmerling, F., & Falkenhagen, J. Identification and classification of technical lignins by means of principle component analysis and k-nearest neighbor algorithm. *Chemistry–Methods*, *1*(8), 354–361.

Huang, D., Liu, C., Zhang, C., Deng, R., Wang, R., Xue, W., Luo, H., Zeng, G., Zhang, Q., & Guo, X. (2019). Cr(VI) removal from aqueous solution using biochar modified with Mg/Al-layered double hydroxide intercalated with ethylenediaminetetraacetic acid. *Bioresource Technology*, *276*, 127–132.

Ilyas, M., Ahmad, W., Khan, H., & Yousaf, S. (2021). Potentially poisonous elements removal from vehicle-wash wastewater and aqueous solutions using composite adsorbents. *Desalination and Water Treatment*, *224*, 331–342.

Imran, M., Khan, Z., U., H., Iqbal, M., M., Iqbal, J., Shah, N. S., Munawar, S., Ali, S., Murtaza, B., Naeem, M. A., & Rizwan, M. (2020). Effect of biochar modified with magnetite nanoparticles and HNO_3 for efficient removal of Cr(VI) from contaminated water: A batch and column scale study. *Environmental Pollution*, *261*, 114231.

Kostryukov, S. G., Matyakubov, H. B., Masterova, Y. Y., Kozlov, A. Sh., Pryanichnikova, M. K., Pynenkov, A. A., & Khluchina, N. A. (2023). Determination of lignin, cellulose, and hemicellulose in plant materials by FTIR Spectroscopy. *Journal of Analytical Chemistry*, *78*(6), 718–727.

Lazaridis, N.K., Bakoyannakis, D.N., & Deliyanni, E.A. (2005). Chromium(VI) sorptive removal from aqueous solutions by nanocrystalline akaganèite. *Chemosphere*, *58*(1), 65–73.

Liu, W., Yang, L., Xu, S., Chen, Y., Liu, B., Li, Z., & Jiang, C. (2018). Efficient removal of hexavalent chromium from water by an adsorption–reduction mechanism with sandwiched nanocomposites. *RSC Advances*, *8*(27), 15087–15093.

Luna, M. S., D., Navarrete, I. A., Adornado, A. P., Tayo, L. L., Soriano, A. N., & Rubi, R. V. D. C. (2023). Influence of nutrient supplement in the single heavy metal (Pb^{2+}, Cd^{2+}, Cr^{3+}) uptake and mineral nutrients absorption by water *Kangkong* (*Ipomoea aquatica forsk*). *Applied Science and Engineering Progress*, 2023, 16(2), 5871.

Mesboua, N., Benyounes, K., Kennouche, S., Ammar, Y., Benmounah, A., & Kemer, H. (2021). Calcinated bentonite as supplementary cementitious materials in cement-based mortar. *Journal of Applied Engineering Sciences*, *11*(1),. 23–32.

Meshram, P., Sahu, S. K., Pandey, B. D., Kumar, V., & Mankhand, T. R. (2012). Removal of chromium(III) from the waste solution of an Indian tannery by amberlite IR 120 resin. *International Journal of Nonferrous Metallurgy*, *1*(3), 32–41.

Nasution, A. N., Amrina, Y., Zein, R., Aziz, H., & Munaf, E. (2015). Biosorption characteristics of Cd(II) ions using herbal plant of mahkota i (Phaleria macrocarpa). *Journal of Chemical and Pharmaceutical Research*, *7*(7), 189–196.

Nguyen, X. P., Nguyen, D. T., Pham, V. V., & Bui, V. D. (2021). Evaluation of the synergistic effect in wastewater treatment from ships by the advanced combination system. *Water Conservation & Management*, *5* (1), 60–65.

Pawar, R. R., Gupta, P., Bajaj, L. H. C. & Lee, S. M. (2016). Al-intercalated acid activated bentonite beads for the removal of aqueous phosphate. *Science of the Total Environment*, *572*, 1222–1230.

Rai, M. K., Giri, B. S., Nath, Y., Bajaj, H., Soni, S., Singh, R. P., Singh, R. S., Rai, & B. N. (2018). Adsorption of hexavalent chromium from aqueous solution by activated carbon prepared from almond shell: Kinetics, equilibrium and thermodynamics study. *Journal of Water Supply: Research and Technology-Aqua*, *67*(8), 724–737.

Rajan, S., Kumar, R., Vivek, S., Gokulan, R., & Balaji, G. (2022). Biosorption of chromium (VI+) using tamarind fruit shells in continuously mixed batch reactor. *Global NEST Journal*, *25*(1), 180–186.

Rezvani, M. A., Afshari, P., & Aghmasheh, M. (2021). Deep catalytic oxidative desulfurization process catalyzed by TBA-PWFe@NiO@BNT composite material as an efficient and recyclable phase-transfer nanocatalyst. *Materials Chemistry and Physics*, *267*, 124662.

Senthilkumar, R., Vijayaraghavan, K., Jegan, J., & Velan, M. (2010). Batch and column removal of total chromium from aqueous solution using Sargassum polycystum. *Environmental Progress & Sustainable Energy*, *29*(3), 334–341.

Kondagorla, S. R., & Madhamshettiwar, S. V. (2024). Adsorption of chromium (VI) from wastewater using blended natural adsorbent. *Oriental Journal Of Chemistry*, *40*(4), 1134–1137.

Slimani, M. S., Aazza, M., Barkouch, H., Amar, M., Alioui, A., Alaoui, O. T., Si Mohamed Bouzzine, S. M., & Ahlafi, H. (2025). Bentonite and organobentonite nanocomposite for removing chromium species from aqueous solutions. *Applied Clay Science*, *267*, 107736.

Song, J., He, Q., Hu, X., Zhang, W., Wang, C., Chen, R., Wang, H., & Mosa, A. (2019). Highly efficient removal of cr(VI) and cu(II) by biochar derived from artemisia argyi stem. *Environmental Science and Pollution Research*, *26*(13), 13221–13234.

Tabak, A., Yilmaz, N., Eren, E., Caglar, B., Afsin, B., & Sarihan, A. (2011). Structural analysis of naproxen-intercalated bentonite (Unye). *Chemical Engineering Journal*, *174*(1), 281–288.

Talukder, P., Sultana, R., Naim, M. R., Turzo, P. I., & Naher, U. H. B. (2024). Optimization of batch process parameters for chromium (VI) removal from synthetic wastewater using eggshell–clay composite. *Discover Applied Sciences*, *6*(6), 291.

Tang, J., Zhao, B., Lyu, H., & Li, D. (2021). Development of a novel pyrite/biochar composite (BM-FeS2@BC) by ball milling for aqueous Cr(VI) removal and its mechanisms. *Journal of Hazardous Materials*, *413*, 125415.

Yang, H., Kim, N. & Park, D. (2023). Superior removal of toxic Cr(VI) from wastewaters by natural pine bark. *Separations*, 1*0*(8), 430.